

Wavelet analysis of x-ray diffraction pattern for glass structures

Yong Ding, Tokuro Nanba, and Yoshinari Miura

*Department of Environmental Chemistry and Materials, Faculty of Environmental Science and Technology, Okayama University,
2-1-1 Tsushima Naka, Okayama-shi 700, Japan*

(Received 14 April 1997; revised manuscript received 8 September 1997)

A wavelet analysis of x-ray diffraction patterns is introduced for analyzing glass structures. The analysis indicates that within a short distance (~ 0.8 nm for silica glass) atoms in the glass are arranged around the most probable positions which are almost as regular as the equilibrium positions in crystal. However, in glass the atomic distribution around the most probable position increases exponentially with increasing interatomic distance (exponentially damped regularity), whereas the crystal does not have this kind of damping. Beyond this distance, it is difficult to determine the structure in atomic scale due to the large atomic distribution. But, the analysis shows that the arrangement of quasiautomatic planes in glass is still statistically regular (with damped regularity) up to an intermediate distance, e.g., 2.5–3.0 nm for silica glass. Then glass structure might be quantitatively determined by means of the structure of corresponding crystals and of the extent of the distributions around the most probable positions for atoms, as well as of the sizes of the structurally correlated group. [S0163-1829(98)04545-7]

I. INTRODUCTION

Crystals have a long-range order characterized by a periodic arrangement of atoms. In contrast, it is generally believed that glasses are lacking this order. Even though the application of glass has a long history, the nature of glass structure has not been totally understood. The inability to resolve glass structure has prevented a clarification of the relationship between properties and structure at the microscopic level. Currently, there are no experimental or mathematical methods to reveal the glass structure with full information.

X-ray diffraction is the most used method for investigating atomic arrangements in crystal. It can also give valuable information about glass structure.^{1,2} By means of the Fourier sine transform of the experimental interference function $sJ_m(s)$ in reciprocal space, a real space differential correlation function $d(r)$, a total correlation function $T(r)$, or a radial distribution function $rdf(r)$ is extracted by the following equations:

$$d(r) = \frac{2}{\pi} \int_0^\infty s J_m(s) \sin sr \, ds, \quad (1a)$$

$$d(r) = 4\pi r[\rho(r) - \rho_0], \quad (1b)$$

$$r \, df(r) = 4\pi r^2 \rho(r), \quad (1c)$$

$$T(r) = 4\pi r \rho(r), \quad (1d)$$

$$s = 4\pi \sin \theta / \lambda, \quad (1e)$$

where $J_m(s)$ is the normalized x-ray diffraction intensity, λ is the wavelength of the x ray, 2θ is the scattering angle, s is the magnitude of scattering vector, $\rho(r)$ is the radial density function of electrons at a distance r from an arbitrarily chosen origin, which is essentially a one dimensional form of crystallographer's Patterson function,³ and ρ_0 is the average radial density. The differential correlation function or radial distribution function is useful to determine interatomic distances and coordination numbers in glass at the short range (< 0.5 nm), evidencing Si-O, O-O, and Si-Si interatomic dis-

tances and the [SiO₄] structural group in silica glass. However, it is believed that these functions are less sensitive at medium (0.5–1 nm) or large distances (> 1 nm).⁴ In order to gain more insight into the glass structure at these large distances, some indirect methods have been established such as structural modeling (such as Zachariasen's random network model⁵ and Lebedev's crystallite model⁶) or simulation by means of molecular dynamics.⁷

Wavelet analysis originated about 15 years ago from a collaboration between Morlet and Grossmann.^{8,9} Wavelet analysis can be defined as an alternative to the classical windowed Fourier analysis.¹⁰ The former will be labeled as a time-scale analysis and the latter is called a time-frequency analysis. In contrast to the Fourier transform, the wavelet transform consists of expanding functions over wavelets which are constructed from a single function $g(r)$ by means of dilation and translation:^{11,12}

$$g_{a,b}(r) = a^{-1/2} g[(r-b)/a], \quad (2)$$

where the parameters a and b can be chosen to vary continuously ($a > 0$), or to be restricted to a discrete lattice. The wavelet transform of a real function $f(r)$ is defined as

$$T_g(a,b) = a^{-1/2} C_g^{-1/2} \int g^*[(r-b)/a] f(r) \, dr, \quad (3)$$

$$C_g = 2\pi \int |\hat{g}(s)|^2 / s \, ds, \quad (4)$$

while the expression in terms of the Fourier transform is

$$T_g(a,b) = a^{1/2} C_g^{-1/2} \int \sin(sb) \hat{g}^*(as) \hat{f}(s) \, ds, \quad (5)$$

where the asterisk denotes the complex conjugate and $\hat{g}(s)$ and $\hat{f}(s)$ are the Fourier transforms of the functions $g(r)$ and $f(r)$, respectively.

Reconstruction of the original function $f(r)$ is given by

$$f(r) = C_g^{-1/2} \int \int a^{-2} T_g(a,b) g_{a,b}(r) da db. \quad (6)$$

A very popular real wavelet is the second derivative of the Gaussian function (i.e., the so-called Mexican hat):

$$g(r) = (1 - r^2) \exp(-r^2/2), \quad (7a)$$

$$\hat{g}(s) = s^2 \exp(-s^2/2), \quad (7b)$$

$$C_g = \pi. \quad (7c)$$

The wavelet transform is seen as a mathematical microscope whose position and magnification are b and $1/a$, respectively, and whose optics is given by the choice of the specific wavelet $g(r)$.¹² The wavelet analysis is related to multiresolution analysis.

This paper is an attempt to introduce the wavelet analysis instead of the Fourier analysis of x-ray diffraction patterns for glass structure, taking silica glass as an example. By means of wavelet analysis of diffraction patterns, some interesting results about the glass structure are obtained.

II. EXPERIMENTAL PROCEDURE

The intensity of x-ray diffraction for an electrically fused silica glass (HERALUX-E glass, SinEtsu Quartz Products Co., Ltd.) was measured with graphite-monochromated Mo $K\alpha$ radiation (50 kV, 200 mA) using a Rigaku Denki RU-200 diffractometer. For comparison, the diffraction patterns of crystalline α cristobalite, synthetic low tridymite (monoclinic phase), and α quartz (Hori Mineralogy, Ltd.) were also obtained under the same experimental conditions ($2\theta = 4 \sim 145^\circ$, step of $2\theta = 0.05^\circ$). The Krough-Moe-Norman method^{13,14} and a least-squares technique¹⁵ to minimize the spurious detail in radial distribution function at small interatomic distance (< 0.1 nm) were used for getting the normalized interference function $sJ_m(s)$.

From Eq. (1a), the Fourier transform of differential correlation function $d(r)$ is $\pi/2 sJ_m(s)$, thus from Eq. (5) the wavelet transform of $d(r)$ is described by

$$T_g(a,b) = a^{1/2} C_g^{-1/2} \pi/2 \int \sin(sb) \hat{g}^*(as) sJ_m(s) ds \quad (8)$$

and $d(r)$ can be reconstructed by means of Eq. (6). Here, we also use the real Gaussian type wavelet $g(r)$ defined in Eq. (7) for analyzing glass structure, as used by Arneodo *et al.*¹² for analyzing the fractal patterns.

III. RESULTS AND DISCUSSION

A. Reciprocal space interference functions and real space atomic correlation functions

Figure 1 shows the x-ray interference functions $sJ_m(s)$ for the silica glass and crystalline α cristobalite, synthetic low tridymite, and α quartz. There are only a few broad interference peaks for the glass, whereas for the crystals a large number of sharp interference peaks are exhibited. This difference results in the damped atomic differential correlation function $d(r)$ for the glass, as shown in Fig. 2, where all differential correlation functions are calculated by Fourier transform in Eq. (1). Figure 2 shows no significant damping for the crystals. We believe that damping of $d(r)$ is the spe-

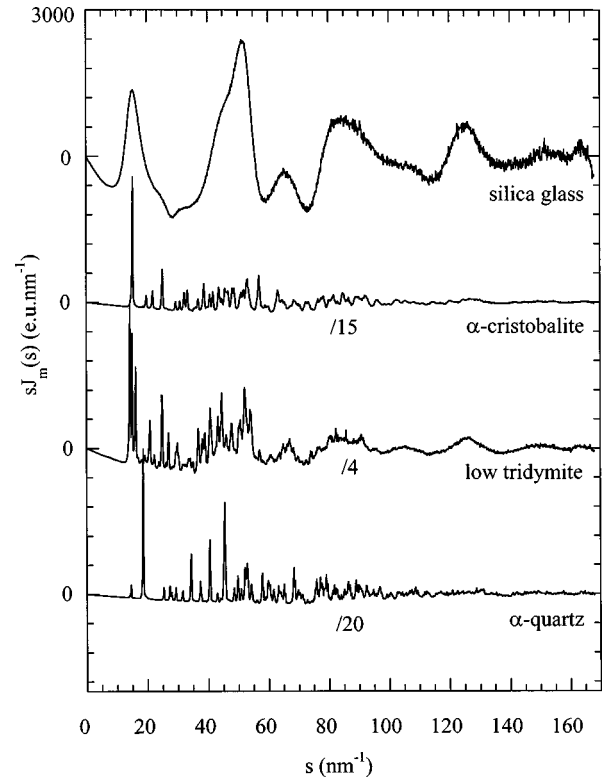


FIG. 1. The x-ray interference functions for silica glass, crystalline α cristobalite, low tridymite, and α quartz.

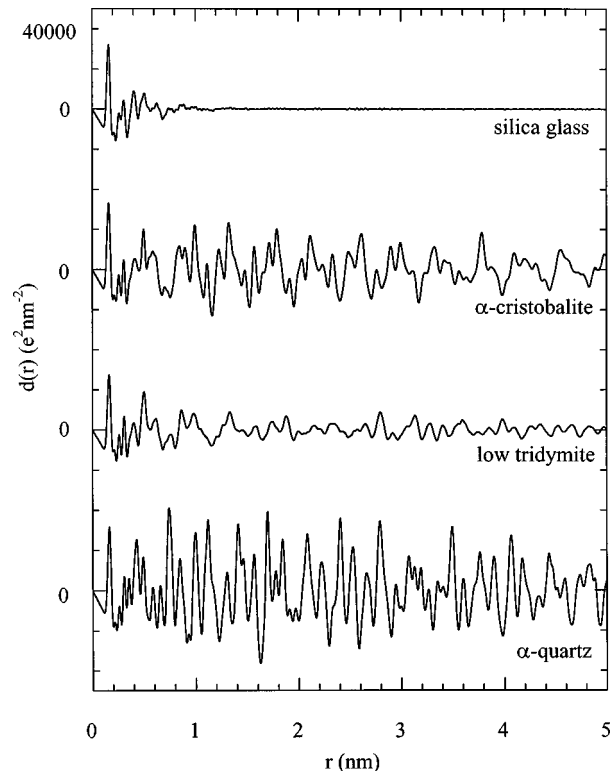


FIG. 2. The x-ray differential correlation functions for silica glass, crystalline α cristobalite, low tridymite, and α quartz, calculated by the Fourier transform of Eq. (1).

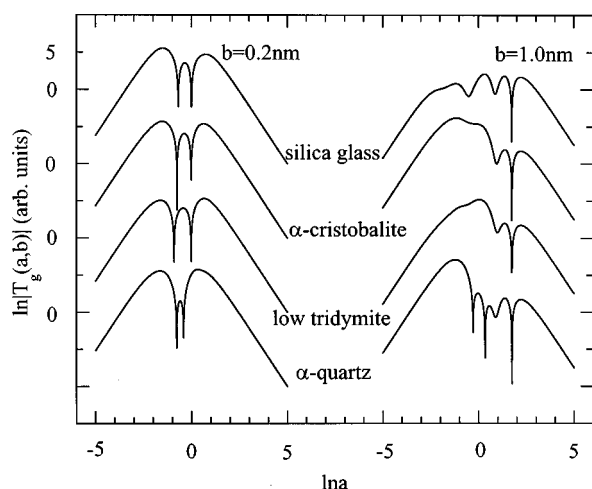


FIG. 3. Wavelet transform $\ln|T_g(a,b)|$ vs $\ln a$ at $b=0.2$ nm and $b=1.0$ nm [defined in Eq. (8)] for the x-ray differential correlation functions of a silica glass, crystalline α cristobalite, low tridymite, and α quartz.

cial characteristic of the glass, which results in the difficulty for glass structure clarification.

Figure 3 shows the absolute value of the wavelet transform $T_g(a,b)$ of $d(r)$ for the silica glass and silica crystals as a function of dilation parameter a for two values of the translation parameter b associated with radial location r (here $b=0.2$ nm and $b=1.0$ nm are shown as examples), plotted in a \ln - \ln scale representative. The oscillation of $|T_g(a,b)|$ represents its magnitude at different scale a for a defined position b . All $\ln|T_g(a,b)|$ s are reduced linearly with $\ln a$ in the two sides, and it is difficult to find any special characteristic for the glass from Fig. 3.

Due to the exponential reduction of $|T_g(a,b)|$ with the parameter $\ln a$ and the localization characteristic of the real Gaussian type wavelet $g(r)$ defined in Eq. (7), it was found that the wavelet-calculated differential correlation function $d(r)$ [obtained using Eq. (6)] is not sensitive to the selection of the integration ranges of a and b when $|\ln a|>2.5$ and $|r-b|>0.3$ nm. Figure 4 compares the Fourier transform $d(r)$ with the wavelet-reconstructed one using integration range $-3<\ln a<3$ and $-0.4\text{ nm}<r-b<0.4\text{ nm}$ ($b>0$) in Eq. (6) for the silica glass and α cristobalite. There is almost no difference between the Fourier transformed $d(r)$ and the wavelet reconstructed one, except the relatively large difference in the short interatomic distance region which is caused by the limited integration range $b\geq 0$. Thus no information was lost using the wavelet reconstruction to obtain the real space correlation functions from the diffraction patterns. Furthermore, the following discussion will show more detailed information about glass structure by means of the multiresolution ability of the wavelet analysis.

B. Multiresolution analysis of differential correlation functions

Using the mathematical microscope, wavelet analysis, the real space correlation function such as $d(r)$ can be decomposed into wavelet transform $T_g(a,b)$ using Eq. (8) with position b and magnification $1/a$ as well as optics $g(r)$. Figures 5(a)–5(d) represent the locations of the maxima of the modulus of the wavelet transforms [referred to as WTMM

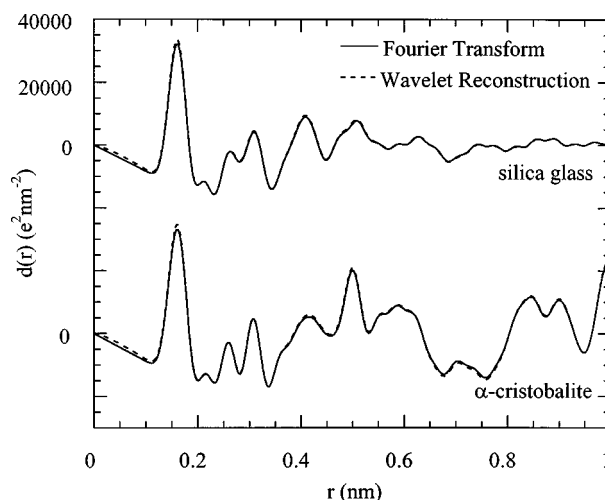


FIG. 4. X-ray differential correlation functions of a silica glass and α cristobalite from Fourier transform (solid lines) and wavelet reconstruction (dashed lines) using the integration range $-3<\ln a<3$ and $-0.4\text{ nm}<r-b<0.4\text{ nm}$ ($b>0$) in Eq. (6).

(Ref. 16)] of $d(r)$ for the silica glass, α cristobalite, low tridymite, and α quartz, respectively. The local maxima lying on connected curves are usually referred to as ‘‘maxima lines.’’^{17,18} Due to the localization characteristic of the wavelet $g(r)$ or $\hat{g}(s)$, the wavelet transform $T_g(a,b)$ of $d(r)$ at larger r are mainly defined by the small scattering vector s , similar to the Fourier transform. By considering the limitation of s in the small scattering range in the present experiments, the maxima lines in the range 0–5 nm are plotted. In Fig. 5, maxima lines in the range of $-2<\ln a<2$ were represented because only a few maxima lines were observed when $\ln a>2$, and a lot of spurious maxima lines related with the ripples in $d(r)$ were observed when $\ln a<-2$.

The wavelet analysis is related to multiresolution analysis. When small a (high resolution, such as $\ln a=-2$) is used, the wavelet detects the locations of WTMM or peak positions associated with interatomic correlation even though some overlapping peaks might still not be separated. Comparing with the maxima lines of the silica crystals in Figs. 5(b)–5(d), the maxima lines of the silica glass in Fig. 5(a) are denser in low $\ln a$ and high b (or r) region (>0.8 nm). Three repeated measurements on the same glass indicated that the maxima lines in the range $b<0.8$ nm reappeared, but those lines in the range of low $\ln a$ and $b>0.8$ nm did not reappear on the same locations, as shown in Fig. 5(e). However, there was almost no change of the maxima lines for the repeated measurements on crystals, as indicated in Fig. 5(f) for three measurements on α cristobalite. These results clearly exhibit the increased randomness of atomic arrangement or atomic overlap for glass in the intermediate range. However, the regularity of maxima lines at the short and medium ranges less than ~ 0.8 nm for the glass is similar to that of the crystals, indicating the short range order as defined by us. At large a (low resolution, such as $\ln a=0$), wavelet does not distinguish the atomic correlation peaks, but the peaks for correlated atomic groups. For understanding what the atomic groups are, the maxima lines in Figs. 5(b)–5(d) for the three silica crystals are investigated. For these crystals, in large $\ln a$ region periodic and straight arrangements of the maxima lines are observed with the periods at $\ln a=0$ shown in Table

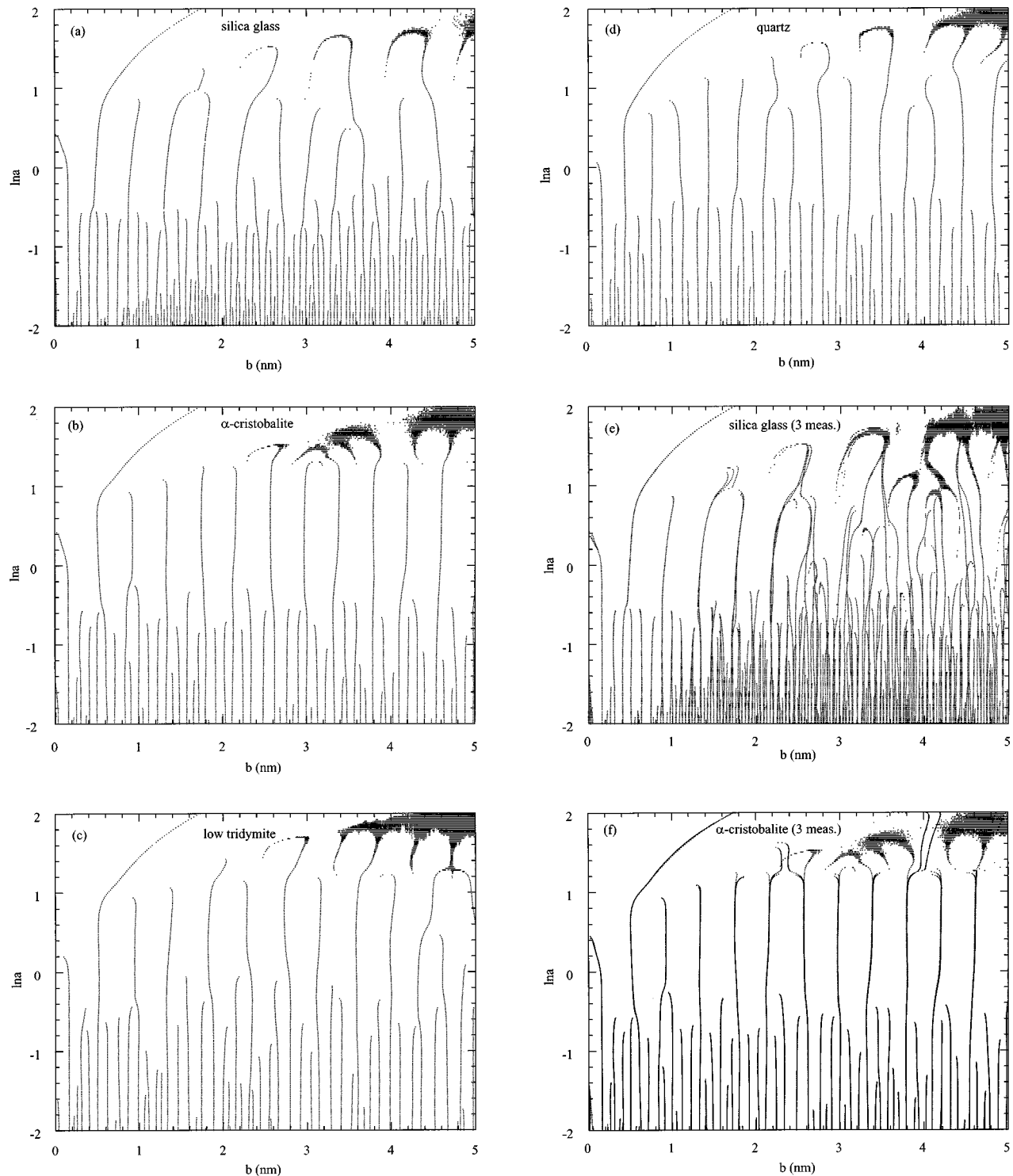


FIG. 5. Locations of the maxima of the moduli of the wavelet transforms or maxima lines of x-ray differential correlation functions for (a) a silica glass, (b) α cristobalite, (c) low tridymite, (d) α quartz, and from three repeated measurements on (e) the silica glass and (f) α cristobalite.

I [(i) the first maximum is excluded during the calculation because it is belonging to the first Si-O interatomic peak which was still detected due to its high intensity and limited integration range $b \geq 0$ in Eq. (8), (ii) the large errors were caused by the low resolution at $\ln a = 0$]. The data in Table I indicate that these periods represent the distances of atomic planes giving the highest x-ray diffraction intensity. Then the wavelet-distinguished correlated atomic group for the crys-

tal at low resolution are the atomic planes with the highest x-ray diffraction ability. It is surprising to find that the maxima lines in the high $\ln a$ region for the glass in Figs. 5(a) and 5(e) are also almost periodic and, moreover, repeated up to an intermediate range (2.5–3.0 nm) for the three measurements. Thus it is considered that the wavelet-distinguished correlated atomic groups at low resolution for the glass might also be related with statistically regular

TABLE I. The periods at $\ln a=0$ in Fig. 5, atomic plane distances d (nm) and Miller indices for the planes with highest x-ray diffraction intensities.

| Substance | Glass | α cristobalite | Low tridymite | α quartz |
|------------------------|--------------------|-----------------------|-------------------------------|-------------------|
| period (nm) | 0.414 ± 0.047 | 0.417 ± 0.031 | 0.405 ± 0.071 | 0.343 ± 0.013 |
| $d(\text{nm}) (I/I_0)$ | 0.418 ± 0.02^a | $0.403974 (100)^b$ | $0.4107 (100), 0.4328 (90)^c$ | $0.3342(100)^d$ |
| Miller index | | (101) | | (101) |

^aCalculated from the first sharp diffraction peak.

^bJCPDS Card No. 39-1425.

^cJCPDS Card No. 18-1170.

^dJCPDS Card No. 33-1161.

atomic planes, or the quasiatomatic planes as defined by us. The above results mean that the arrangement in the atomic group or plane scale in a glass still has a statistical regularity extending to the intermediate range even though it is difficult to detect the regularity in atomic scale in this range. In other words, atoms are still statistically distributed around the quasiatomatic planes even though there are a large fluctuation for atomic positions in the intermediate range. Furthermore, it is interesting to note that the period 0.414 nm for the silica glass is near the calculated atomic plane distance 0.418 nm from the first sharp diffraction peak. Then it is reasonable that there are statistically regular planes in glass, the so-called quasi-Bragg planes.^{19–21} The quasiatomatic plane having highest x-ray diffraction ability is associated with the first sharp diffraction peak.

In order to exactly understand the structural characteristic for glass, Figs. 6(a)–6(c) compare the $T_g(a, b)$ of $d(r)$ of the silica glass with those of the three silica crystals for $\ln a=2$, $\ln a=1$, and $\ln a=0$, respectively. At small and medium $\ln a$, $T_g(a, b)$ basically represents the profile of the atomic correlation, similar to the profile of $d(r)$ in Fig. 2, even though some weak peaks such as the first O-O peak (at ~ 0.263 nm) are lost at medium $\ln a$. At large $\ln a$, $T_g(a, b)$ represents the correlation of the atomic planes having the highest x-ray diffraction intensity. For a crystal a strong correlation can be clearly observed up to long range due to the periodic or regular arrangement of atoms and atomic planes. For a glass, even though the peaks of the correlation function can be detected up to intermediate range by the wavelet analysis as shown in Fig. 5(a), the peak intensities damp dramatically with increasing interatomic distances. From Figs. 6(a) and 6(b), it is difficult to mathematically describe the damping characteristics of a glass due to the complex vibration. However, the vibration in Fig. 6(c) seems to be simple. Figure 7 plots the logarithmic peak intensity of $T_g(a, b)$, $\ln T_g^p(a, b)$ at $\ln a=0$, as a function of b (the first peak is excluded again). It is found that $\ln T_g^p(a, b)$ at $\ln a=0$ are almost constants with increasing b for the crystals, but decrease exponentially for the glass up to ~ 3.0 nm. This relationship can be expressed by

$$T_g^p(a, b) = \Gamma \exp(-b/\beta) \quad (\ln a = 0) \quad (9a)$$

or

$$\ln T_g^p(a, b) = \ln \Gamma - b/\beta \quad (\ln a = 0), \quad (9b)$$

where Γ is the pre-exponential factor, and β is called the characteristic correlation length. For crystal, β is a very large

or infinite value. The peak value of $T_g(a, b)$ at $\ln a=0$ for a crystal, $T_g^{cp}(a, b)$, could be expressed by

$$T_g^{cp}(a, b) = \Gamma \quad (\ln a = 0). \quad (9c)$$

Then for glass,

$$T_g^p(a, b) = T_g^{cp'}(a, b) \exp(-b/\beta) \quad (\ln a = 0), \quad (9d)$$

where $T_g^{cp'}(a, b)$ is the peak value of $T_g(a, b)$ of a corresponding crystal associated with the glass.

For the silica glass the β estimated in $\ln a=0$ is only 0.336 nm. This phenomenon means that for glass the correlation of the quasiatomatic planes decrease dramatically with increasing distances, whereas for crystals the atomic planes are still strongly correlated at long range with a very long or infinite characteristic correlation length. According to the definition of differential correlation function in Eq. (1), an exponentially damped correlation defines the exponentially increased distribution of interatomic plane distances. The difference in correlation lengths or distribution is the main structural difference between the glass and crystals, which is mathematically described in Eq. (9).

Another characteristic indicated in Fig. 7 is the levelling off of the logarithmic decrease of $T_g^p(a, b)$ for b larger than ~ 3.0 nm (repeated measurements for the same sample gave a broad range of 3.0 ± 0.5 nm, also in Fig. 7). Beyond this range, $T_g^p(a, b)$ appeared random. This range might be the diameter of a structurally correlated group or particle. There is structural correlation inside the particle, and there is little or no correlation outside the particle. The size was very sensitive to the experimental interference function $sJ_m(s)$ in the small s region. Due to the difficulty of the measurement of $sJ_m(s)$ in the small s region, the exact size might be larger or smaller than 2.5–3.0 nm, which should be further investigated.

Furthermore, it is found that in low resolution region (large a region such as $\ln a \sim 0$ in Fig. 5), the data in Fig. 7 are not sensitive to $\ln a$, as shown in Fig. 8 for the data with $\ln a=0.2-0.4$ with a step 0.2 for α cristobalite and the silica glass (for the glass a few data with very small values such as the data for $b \sim 2.4$ nm, which still represents the atomic correlation, are not plotted here). Then, it could be expected that Eq. (9) would be applicable to other $\ln a$ and b . In this case we have the following equation for the glass:

$$T_g(a, b) = T_g^c(a, b) \exp(-b/\beta), \quad (10)$$

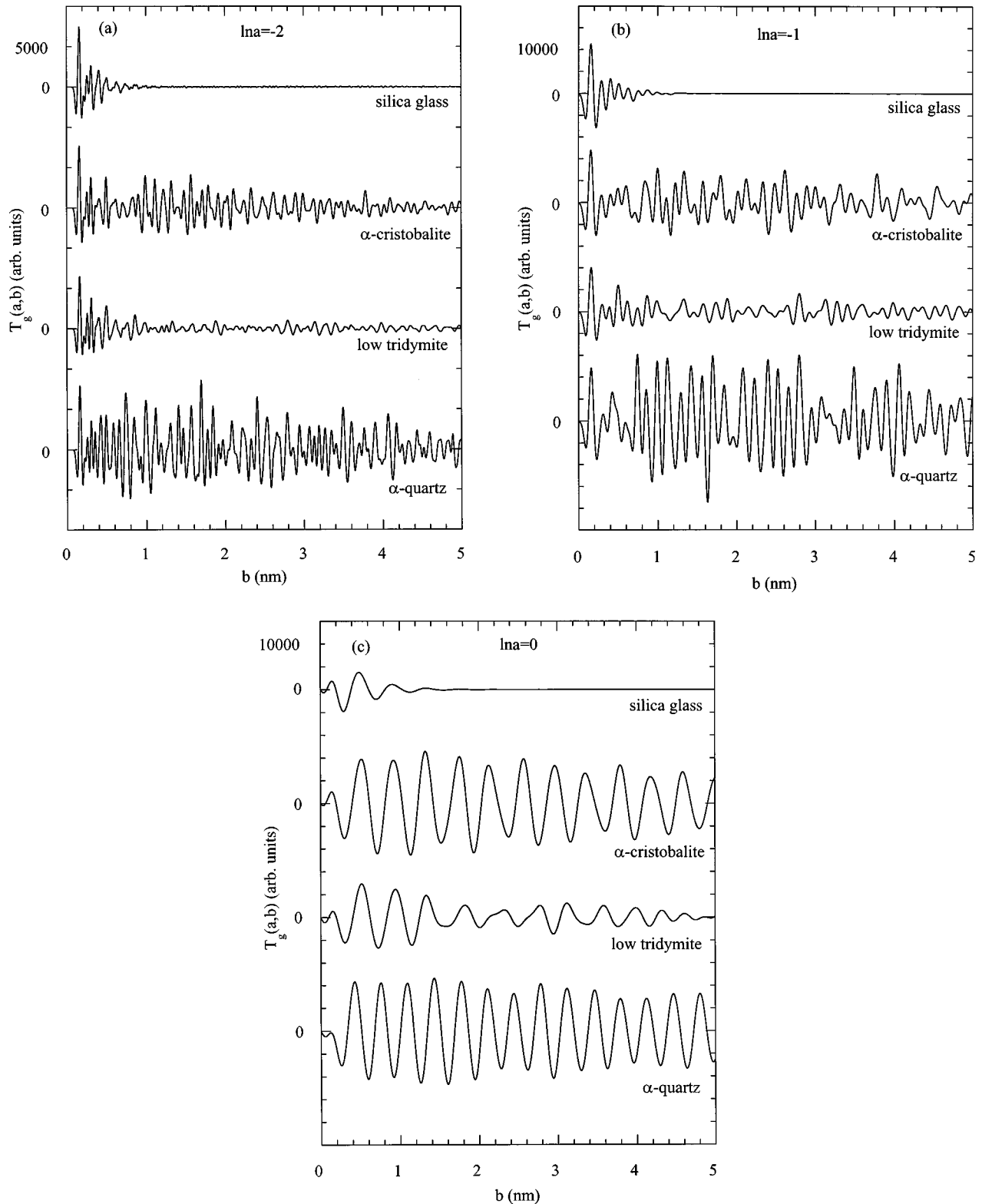


FIG. 6. Wavelet transform $T_g(a,b)$ vs b of the x-ray differential correlation functions for a silica glass, crystalline α cristobalite, low tridymite, and α quartz at (a) $\ln a = -2$, (b) $\ln a = -1$, (c) $\ln a = 0$.

where $T_g^c(a,b)$ is similar to the $T_g(a,b)$ for crystal, and it is the wavelet transform of a corresponding crystal associated with the glass.

From wavelet reconstruction using Eq. (6) and $T_g(a,b)$ in Eq. (10), the relationship between the atomic differential correlation function $d(r)$ of a glass and that of its corresponding crystal $d_c(r)$ can be expressed by

$$d(r) = \alpha \exp(-r/\beta) d_c(r), \quad (11)$$

where α is a calibration factor (~ 1), which is required because there should be no damping for the correlation function within the first interatomic distance and other factors such as the periodic difference between glass and crystal should be considered. β is the characteristic correlation

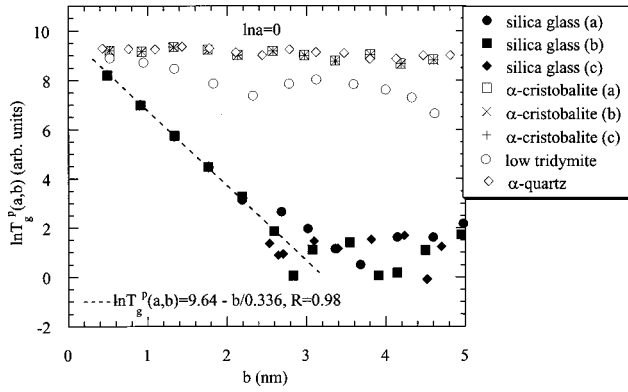


FIG. 7. Logarithmic peak intensity of $T_g(a,b)$, $\ln T_g^p(a,b)$ vs b at $\ln a=0$ for silica glass and crystalline α cristobalite measured for three times (a)–(c), and low tridymite and α quartz.

length for the atomic arrangement in glass, which determine the extent of atomic distribution or damped regularity. β is related to the distance at which the atomic correlation in glass is $\sim 1/e$ of that in the corresponding crystal.

C. Glass structure from wavelet analysis

From the above results and discussion, it can be imagined that within a short distance (including short and medium range, ~ 0.8 nm for the silica glass) there is a statistical atomic scale order in glass for which the atoms are arranged around the most probable positions which are also regular or periodic. Their arrangement is similar to that of the equilibrium positions for the atoms in crystals. We define this as short range order. The only difference between crystal and glass in the short range is the degree of atomic displacement around the equilibrium positions, as indicated in the wavelet transform of the differential correlation functions in Figs. 6 and 7. For crystal, the atoms are periodically located at the equilibrium positions with displacement only due to thermal vibrations. But for glass, the atoms are arranged around the most probable positions or equilibrium positions which are periodic with distributions increasing exponentially with in-

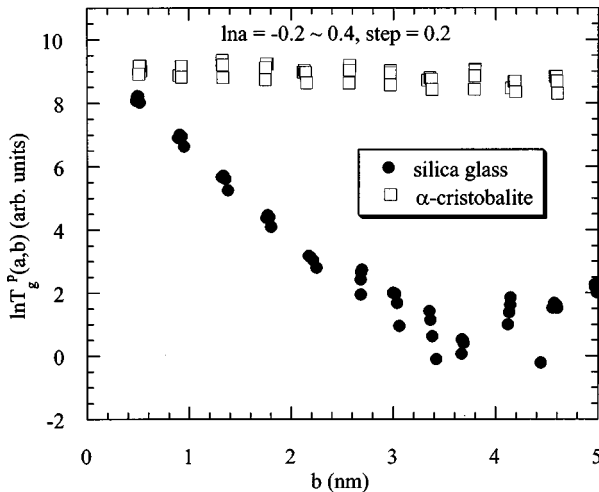


FIG. 8. Logarithmic peak intensity of $T_g(a,b)$, $\ln T_g^p(a,b)$ vs b at $\ln a = -0.2 \sim 0.4$ with a step 0.2 for a silica glass and crystalline α cristobalite.

TABLE II. Estimated α , β , and R_χ^X in $0.1 \leq r \leq 0.8$ nm.

| Assumed corresponding crystal | α | β (nm) | R_χ^X (%) |
|-------------------------------|----------|--------------|----------------|
| α cristobalite | 1.43 | 0.397 | 5.89 |
| low tridymite | 1.53 | 0.473 | 6.83 |
| α quartz | 1.86 | 0.208 | 12.47 |

creasing interatomic distances. Beyond the short range, it is difficult to determine the structure at an atomic scale due to the large interatomic distance fluctuation. However, the most probable locations of the quasiautomatic planes in glass are still periodic up to an intermediate range (2.5–3.0 nm for the silica glass). We define this as intermediate range order. The only difference for the arrangement of atomic planes between crystal and glass in the intermediate range is again the degrees of distribution of the atomic planes around the equilibrium or most probable positions. Beyond the intermediate range, there is almost no correlation for atomic or atomic plane positions. So this intermediate range might be an average size (diameter) of atomic groups or particles whose atomic positions are statistically correlated.

There have been a lot of glass structure models,^{5,6,22–25} and two representative models are Zachariasen's random network model⁵ and Lebedev's crystallite model.⁶ But, there are still many discrepancies among them. Our wavelet analysis indicates that there is a similarity in the atomic structures of glasses and crystals in statistical means, but the atomic randomness in glass increases exponentially with interatomic distance. The extent of randomness in a glass structure might be expressed mathematically with the characteristic correlation length β in Eqs. (9)–(11). These results conceptually support the modified crystallite models such as the quasi-crystalline model^{22,23} or paracrystalline model.²⁴ But a new model for glass structure might be required for a better and quantitative understanding of the complex glass structure and the structural relations of various properties. This kind of research is under way.

D. Estimation of structural parameters of glass

Here is the preliminary estimation of the structural parameters of the silica glass at the atomic scale. Taking the measured $d(r)$ of the silica glass and assuming successively $d_c(r)$ from the crystals α quartz, low tridymite, and α cristobalite, a least-square refinement of Eq. (11) is conducted in a range $0.1 \leq r \leq 0.8$ nm. This gives the estimated α , β , and the discrepancy factor R_χ^X defined in Ref. 26 (the superscript X means that the discrepancy factor R_χ is for x-ray diffraction) for the total correlation function $T(r)$ in Eq. (1) as listed in Table II. Here the density of silica glass 2.20 g/cm³ is used for calculation of the average radial density ρ_0 even for the crystals.

From the results in Table II, it is clear that the discrepancy factor is larger when α quartz is used as the corresponding crystal. The discrepancy factors for low tridymite and α cristobalite are similar. These two discrepancy factors are comparable with the molecular dynamic simulation result $R_\chi^N = 6.8\%$ (a very good simulation, the superscript N means that R_χ is for neutron diffraction) in the same r range.^{26,27}

For comparison, Fig. 9 shows the measured x-ray radial distribution function of the silica glass and the calculated functions using Eq. (11) when α quartz, low tridymite, and α cristobalite are used as the corresponding crystals. This is just a preliminary estimation, and it cannot be concluded which one is the corresponding crystal for silica glass. It is also possible that another crystalline phase such as a high temperature cristobalite or tridymite phase of silica will be the corresponding crystal. But the above estimation indicates that Eq. (11) from wavelet analysis might give a suitable mathematical description for glass structure. Further searching and refinement of the structural parameters of the corresponding crystal should be conducted.

The searching for corresponding crystals for glass should be done by further refinement of the structural parameters of the corresponding crystals, parameters α and β in Eqs. (10) and (11), which might be realized in a similar way with the Rietveld method^{28,29} for the refinement of the structural parameters of crystal. The Rietveld method is a least-square refinement method for the measured and calculated diffraction patterns. At present, we are developing a refinement method for the measured differential correlation function of glass and the calculated one of the corresponding crystal according to Eqs. (10) and (11).

IV. CONCLUSIONS

The multiresolution wavelet analysis is a unique technique for giving a deep understanding of the glass structure. The analysis indicates that there are two length scales for glass structure, named short and intermediate ranges. In the short range (~ 0.8 nm for a silica glass) atoms in glass are arranged around the most probable positions which are almost as regular as the equilibrium positions in crystal, with fluctuations of the interatomic distances increasing exponentially with increasing interatomic distances (statistical regularity). Beyond the short range, it is difficult to determine the structure in atomic scale due to the large fluctuations of interatomic distances. However, up to an intermediate range (2.5–3.0 nm for silica glass) the arrangement of quasicrystalline planes in glass is still statistically regular and periodic. This intermediate range is considered as the sizes (diameters) of the structurally correlated group. The analysis indicates that glass structure might be determined by means of the struc-

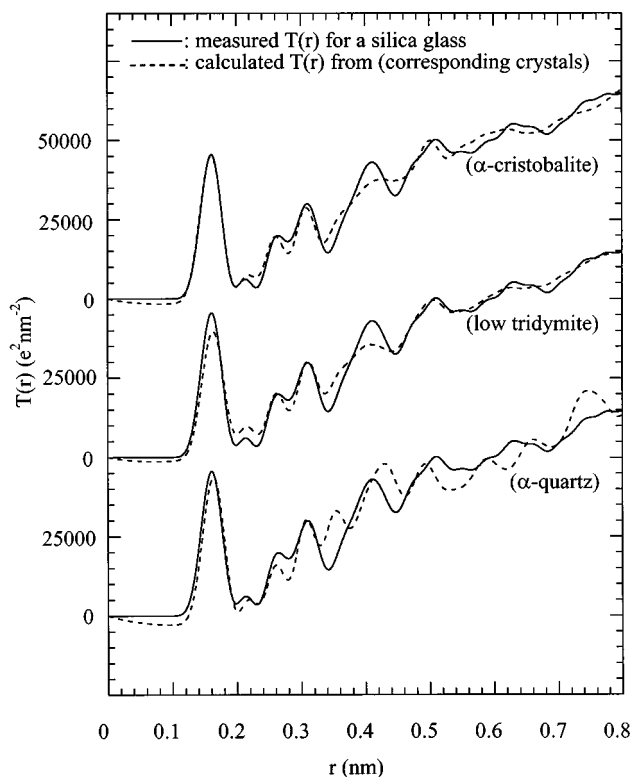


FIG. 9. A comparison of the measured x-ray total correlation function of a silica glass (solid line) and the calculated functions from Eq. (11) and Eq. (1) when α quartz, low tridymite, and α cristobalite are assumed as the corresponding crystals (dashed lines).

ture of corresponding crystals and the extent of the distribution around the most probable positions for atoms, as well as the sizes of the structurally correlated group.

ACKNOWLEDGMENTS

The authors are grateful to Dr. A. Osaka, Dr. P. H. Gaskell, and Dr. M. Affatigato for constructive comments and valuable discussions. Dr. M. Affatigato is also acknowledged for his help in revising the English of the paper. The authors would also like to thank SinEtsu Quartz Products Co., Ltd for providing the silica glass specimens for the research.

¹R. L. Mozzi and B. E. Warren, *J. Appl. Crystallogr.* **2**, 164 (1969); **3**, 251 (1970).

²A. C. Wright, in *Experimental Techniques of Glass Science*, edited by C. J. Simmons and O. H. El-Bayoumi (The American Ceramics Society, Westerville, OH, 1993), p. 205.

³M. F. C. Ladd and R. A. Palmer, *Structure Determination by X-ray Crystallography*, 3rd ed. (Plenum, New York, 1993), p. 278.

⁴R. Elliott, *J. Non-Cryst. Solids* **182**, 1 (1995).

⁵W. H. Zachariasen, *J. Am. Chem. Soc.* **54**, 3841 (1932); *Glastech. Ber.* **11**, 120 (1933).

⁶A. A. Lebedev, *Trudy Gosud. Optichesk. Inst. Leningrad* **2** (10), (1921); *Bull. Acad. Sci. USSR, Phys. Ser.* **4**, 584 (1940).

⁷J. P. Rino and I. Ebbsjo, *Phys. Rev. B* **47**, 3053 (1993).

⁸J. Morlet, G. Arens, E. Fourgeau, and D. Giard, *Geophysics* **47**, 203 (1982).

⁹A. Grossmann and J. Morlet, in *Mathematics and Physics*, Vol. 1 of Lectures on Recent Results, edited by L. Streit (World Scientific, Singapore, 1985).

¹⁰Y. Meyer, in *Progress in Wavelet Analysis and Application*, edited by Y. Meyer and S. Rogues (Editions Frontières, France, 1993), p. 9.

¹¹F. Argoual, A. Arneodo, J. Elezgaray, and G. Grasseau, *Phys. Rev. A* **41**, 5537 (1990).

¹²A. Arneodo and G. Grasseau, *Phys. Rev. Lett.* **61**, 2281 (1988).

¹³J. Krogh-Moe, *Acta Crystallogr.* **9**, 951 (1956).

¹⁴N. Norman, *Acta Crystallogr.* **10**, 370 (1957).

¹⁵J. H. Konnert and J. Karle, *Acta Crystallogr., Sect. A: Cryst.*

- Phys., Diffr., Theor. Gen. Crystallogr. **29**, 702 (1973).
- ¹⁶A. Arneodo, F. Argoul, J. F. Muzy, M. Tabard, and E. Bacry, *Fractals* **1**, 629 (1993).
- ¹⁷S. Mallat and S. Zhong, *IEEE Trans. Pattern. Anal. Mach. Intell.* **14**, 710 (1992).
- ¹⁸S. Mallat and W. L. Hwang, *IEEE Trans. Inf. Theory* **38**, 617 (1992).
- ¹⁹A. P. Sokolov, A. Kisliuk, M. Soltwisch, and D. Quitmann, *Phys. Rev. Lett.* **69**, 1540 (1992).
- ²⁰A. Uhlherr and S. R. Elliott, *J. Non-Cryst. Solids* **192&193**, 98 (1995).
- ²¹P. H. Gaskell and D. J. Wallis, *Phys. Rev. Lett.* **76**, 66 (1996).
- ²²P. L. Maitrepierre, *J. Appl. Phys.* **40**, 4826 (1969).
- ²³A. J. Leadbetter and A. C. Wright, *J. Non-Cryst. Solids* **7**, 23 (1972).
- ²⁴R. Hosemann, M. P. Hentschel, U. Schmeisser, and R. Brückner, *J. Non-Cryst. Solids* **83**, 223 (1986).
- ²⁵P. H. Gaskell, *J. Non-Cryst. Solids* **32**, 207 (1979).
- ²⁶A. C. Wright, *J. Non-Cryst. Solids* **159**, 264 (1993).
- ²⁷B. Vessal, M. Amini, and C. R. A. Catlow, *J. Non-Cryst. Solids* **159**, 184 (1993).
- ²⁸H. M. Rietveld, *J. Appl. Crystallogr.* **2**, 65 (1969).
- ²⁹H. M. Rietveld, *Acta Crystallogr.* **22**, 151 (1967).